PRZEGLĄD ELEKTROTECHNICZNY

Ukazuje się od 1919 roku 1'11

Organ Stowarzyszenia Elektryków Polskich • Wydawnictwo SIGMA-NOT Sp. z o.o.

Helmo K. MORALES PAREDES[1], Alessandro COSTABEBER[2], Paolo TENTI[2]

University of Campinas, Brazil (1), University of Padova, Italy (2)

Application of Conservative Power Theory to cooperative control of distributed compensators in smart grids

Abstract. *Smart grids are characterized by the availability of distributed energy resources (DER), including power switching interfaces (PSI) to connect to the grid. This creates a new scenario for the management of power grids, because DER increase the power capability and flexibility of the network at the expense of a higher complexity of control. If properly driven, however, PSI can improve power quality and distribution efficiency. On the contrary, every control misbehavior can cause voltage instability and/or circulation of useless currents, with the risk to affect network operation. Moreover, especially in case of islanded operation, smart grids can suffer from voltage distortion, asymmetry, and frequency variations, which may affect control accuracy and stability. In such a context, a cooperative control approach of PSI and any other electronic power processors (EPP) acting in the grid is needed, to ensure proper network operation even under severely disturbed conditions. This paper shows that the Conservative Power Theory (CPT) provides a viable background for the development of an optimum control technique of distributed EPP.*

Streszczenie. *Inteligentne sieci elektroenergetyczne charakteryzują się dostępnością rozproszonych źródeł energii (DER) wraz z urządzeniami pośredniczącymi (PSI) łączącymi je do sieci energetycznej. Tworzy to nowe warunki zarządzania siecią energetyczną, gdyż DER powiększa moc i elastyczność systemu, jednak kosztem wzrostu złożoności jego sterowania. Prawidłowo sterowany PSI może jednak poprawić jakość energii i sprawność jej dystrybucji. W przeciwnym przypadku, niewłaściwie sterowanie PSI może spowodować niestabilność napięcia i/lub przepływy bezużytecznych prądów, wraz z ryzykiem wpływu na pracę sieci. Ponadto w sieci inteligentnej, szczególnie w warunkach pracy izolowanej, może pojawić się odkształcenie napięcia, asymetria oraz wahania częstotliwości, co może oddziaływać na dokładność sterowania i stabilność systemu. Aby zagwarantować właściwą pracę sieci, nawet w mocno zaburzonych warunkach, potrzebne jest współzależne sterowanie PSI i innych procesorów mocy (EPP). Niniejszy artykuł pokazuje, że Zachowawcza Teoria Mocy (CPT) tworzy realną podstawę do rozwoju optymalnej techniki sterowania rozproszonych EPP.* ***(Zastosowanie zachowawczej teorii mocy do współzależnego sterowania kompensatorów rozproszonych w sieciach inteligentnych)***

Keywords: Smart grid, Renewable energy, Distributed energy resources, Distributed control, Conservative power theory, Electronic power processors.
Słowa kluczowe: inteligentne sieci elektroenergetyczne, energia odnawialna, rozproszone zasoby energii, sterowanie rozproszone, zachowawcza teoria mocy, elektroniczne procesory mocy.

Introduction

In recent years, the adoption of "green energy" policies in several countries encouraged installation of small- or medium-power *DER*, including renewable or alternative energy sources and storage elements. Since every unit of this kind is equipped with an *SPC*, we assist to the proliferation of "intelligent power sources". This is the technical essence of smart grids, where intelligent power sources cooperate to meet the energy demand by exploiting renewable energy at the maximum extent.

The smart grid paradigm is therefore different from the traditional one, based on the assumption of few power sources of large capacity. Moreover, while traditionally every apparatus connected to the grid is devised to suit local needs, assuming no interaction with the rest of the network, in smart grids the distributed power sources interact each other and with the rest of the network. Every action to improve grid operation (power flow control, voltage support, unbalance compensation, harmonic mitigation) must therefore be coordinated among all electronic power processors (*EPP*) acting in network, i.e.:

- Switching Power Converters (*SPC*), which include Power Switching Interfaces (*PSI*) and Active Power Filters (*APF*);
- Static *VAR* Compensators (*SVC*), which include Thyristor Controlled Reactors (*TCR*), Thyristor switched capacitors (*TSC*) and *STATCOM* (low-frequency switching reactive compensators).

From the control perspective, we must take into account that EPP tend to interact through distribution lines, possibly causing control instabilities. Moreover, they are normally designed for sinusoidal supply and their operation can be affected by voltage distortion.

From the above considerations it follows that facing the problems of smart grids requires a comprehensive approach to cooperative operation of *EPP* [1-3]. A revision of *EPP* control strategy is needed, since they must operate under non-sinusoidal conditions [4-19] and perform local [7,11,15-17] and global [3] duties at the same time, by interacting with each other and with remote network controllers. The control architecture must support global and local optimization needs, while allowing full exploitation of *DER* and of the existing distribution infrastructure.

This paper presents an approach to cooperative control of distributed *EPP* which is based on the *CPT* [8]. It makes use of conservative power terms as control variables, and allows optimization of network operation by proper sharing of control duties among *EPP*.

Control of electronic power processors by power and energy commands

In the following, reference will be made to the symbols and results presented in [8]. Moreover, for control purpose we

define the instantaneous "power/energy" vector command in the network port as:

$$[s] = [\underline{u} \circ \underline{i} \quad \underline{\hat{u}} \circ \underline{i}] = [p \quad w] \tag{1}$$

where $\underline{u}$, $\underline{i}$ are the vectors of voltages and currents at that and $\underline{\hat{u}}$ is called unbiased voltage integral. Term w is called *instantaneous reactive energy*.

The equivalent single-phase representation of a smart grid, or a section of it, is shown in Fig.1. *EPP* and *PCC* terminals are shown separately, while the other network components (distribution lines, transformers, loads, etc.) are included in box π.

TSC are made of a set of capacitor banks, controllable stepwise, while *TCR* are delta-connected variable inductors, controlled independently. Their capabilities are different, since *TSC* are normally used for reactive compensation only [9], while *TCR* can contribute to unbalance compensation too [9]. *SPC*, which perform as wideband controllable current sources, can perform every type of function, including harmonic mitigation. The duties of *TCR* and *TSC* are performed by *STATCOM* too.

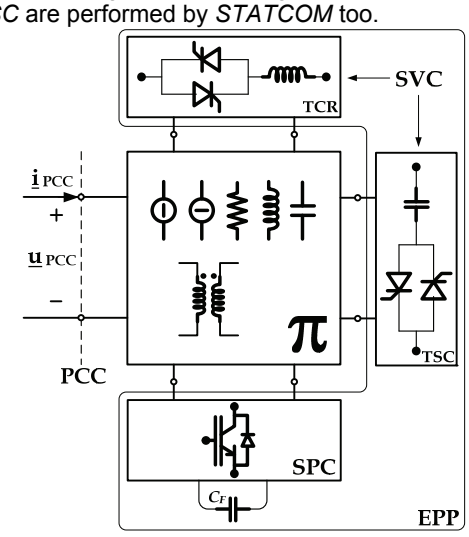

Fig. 1. General representation of a smart grid

In this section we analyze the *EPP* control methods under the assumption that they are driven by suitable complex power commands, either average or instantaneous.

We will make reference to sequence components [10] which, for given three-phase variables x, are given by:

- Positive sequence:

$$\underline{x}^p = \begin{cases} x_1^p(t) = \dfrac{x_1(t) + x_2(t + T/3) + x_3(t + 2T/3)}{3} \\ x_2^p(t) = x_1^p(t - T/3) \\ x_3^p(t) = x_1^p(t - 2T/3) \end{cases} \tag{2.a}$$

- Negative sequence:

$$\underline{x}^n = \begin{cases} x_1^n(t) = \dfrac{x_1(t) + x_2(t - T/3) + x_3(t - 2T/3)}{3} \\ x_2^n(t) = x_1^p(t + T/3) \\ x_3^n(t) = x_1^p(t + 2T/3) \end{cases} \tag{2.b}$$

In the special case of sinusoidal variables, the sequence components can be expressed by:

- Positive sequence:

$$\underline{x}^p = \sqrt{2}\, X^p \begin{vmatrix} \sin(\omega t + \chi^p) \\ \sin(\omega t + \chi^p - 2\pi/3) \\ \sin(\omega t + \chi^p - 4\pi/3) \end{vmatrix} \tag{3.a}$$

- Negative sequence:

$$\underline{x}^n = \sqrt{2}\, X^n \begin{vmatrix} \sin(\omega t + \chi^n) \\ \sin(\omega t + \chi^n + 2\pi/3) \\ \sin(\omega t + \chi^n + 4\pi/3) \end{vmatrix} \tag{3.b}$$

The instantaneous "power/energy" vector associated to positive-sequence voltage vector $\underline{u}^p$ (of phase α^p) and positive-sequence current vector $\underline{i}^p$ (of phase β^p), according to (1), is given by:

$$\begin{aligned} [s^p] &= [P^p \quad W^p] \\ P^p &= 3U^p I^p \cos(\alpha^p - \beta^p) = 3U^p I^p \cos\varphi^p \\ W^p &= 3\hat{U}^p I^p \sin(\alpha^p - \beta^p) = 3\hat{U}^p I^p \sin\varphi^p \end{aligned} \tag{4.a}$$

where, U^p and I^p are rms values of voltages and currents, P^p and W^p are active power and reactive energy, and φ^p is phase displacement between vectors $\underline{u}^p$ and $\underline{i}^p$.

Instead, the instantaneous "power/energy" vector associated to positive-sequence voltage vector, $\underline{u}^p$ (of phase α^p) and negative-sequence current vector $\underline{i}^n$ (of phase β^n) is:

$$\begin{aligned} [s^n] &= [p^n \quad w^n] = -[3U^p I^n \quad 3\hat{U}^p I^n] e^{j(2\omega t + \alpha^p + \beta^n)} \\ p^n &= -3U^p I^n \cos(2\vartheta - \varphi^n) \\ w^n &= -3\hat{U}^p I^n \sin(2\vartheta - \varphi^n) \end{aligned} \tag{4.b}$$

where $\vartheta = \omega t + \alpha^p$ is angular position of voltage vector and φ^n is phase displacement between voltage u_1^p and current i_1^n of phase 1.

TSC operation and control

TSC can be represented by three symmetrical capacitors, wye- or delta-connected, and are made up of a set of parallel branches, each one including a thyristor-switched capacitor bank. The equivalent phase capacitance can be varied stepwise in the range $0 \le C \le C_{max}$.

For control purpose, we assume that supply voltages are purely sinusoidal and symmetrical with positive sequence. In fact, the other voltage components are useless for reactive power control, which is the main function of *TSC*, and can be neglected. In practice, they cause unwanted currents, which are compensated by other compensation devices (*SPC*).

The positive-sequence currents absorbed by the *TSC* have a phase displacement of $+\pi/2$ and their rms value is:

$$I_C^p = \omega C U^p \tag{5.a}$$

The corresponding reactive power, is:

$$Q_C^p = -3\, U^p I_C^p = -3\omega C {U^p}^2 \tag{5.b}$$

Thus, given a reactive power command the value of the equivalent capacitor is immediately determined by (5.b).

TCR operation and control

TCR can be represented by delta-connected susceptances B_{12}, B_{23}, B_{31}. Each branch is made up of a fixed inductor L in series with a phase-controlled thyristor

switch, so that its susceptance can be regulated in the range $0 \le B \le B_{max}$, where $B_{max} = 1/L$.

Also in this case we assume that supply voltages are purely sinusoidal and symmetrical of positive sequence, since the other voltage components are useless for reactive power and unbalance control. Their effect can be compensated, together with the current harmonics generated by *TCR*, by switching compensators *SPC/APF*.

Given B_{12}, B_{23}, B_{31}, the line currents absorbed by the *TCR* are given by:

(6.a) $$\underline{i}_B = \begin{vmatrix} B_{12}+B_{31} & -B_{12} & -B_{31} \\ -B_{12} & B_{12}+B_{23} & -B_{23} \\ -B_{31} & -B_{23} & B_{31}+B_{23} \end{vmatrix} \cdot \underline{\hat{u}}^p$$

where $\underline{\hat{u}}^p$ are the positive-sequence unbaised voltage integrals.

TCR currents can be divided into positive- and negative-sequence components, which are independently used for reactive and unbalance compensation.

Reactive compensation by positive-sequence currents

Positive-sequence currents are derived by applying transformation (2.a) to currents $\underline{i}_B$. The result is:

(7.a) $$\underline{i}_B^p = \left(B_{12}+B_{23}+B_{31}\right)\underline{\hat{u}}^p = B_0\,\underline{\hat{u}}^p$$

where B_0 is total susceptance. The rms value of positive-sequence currents is:

(7.b) $$I_B^p = \frac{B_0}{\omega} U^p$$

Thus:

(7.c) $$Q_B^p = 3U^p I_B^p = 3U^{p\,2}\,\frac{B_0}{\omega}$$

The symmetrical susceptances needed to compensate for reactive power Q_B^p are therefore given by:

(7.d) $$B_{12} = B_{23} = B_{31} = B_B^p = \frac{B_0}{3} = \omega\frac{Q_B^p}{9U^{p\,2}}$$

Unbalance compensation by negative-sequence currents

Negative-sequence currents are derived by applying transformation (2.b) to currents $\underline{i}_B$. The result is:

(8.a) $$\underline{i}_B^n = -\begin{vmatrix} B_{23} & B_{12} & B_{31} \\ B_{12} & B_{31} & B_{23} \\ B_{31} & B_{23} & B_{12} \end{vmatrix} \cdot \underline{\hat{u}}^p$$

Note that currents $\underline{i}_B^n$ do not change by adding the same quantity to all susceptances. Let's therefore assume arbitrarily $B_{31} = 0$. The instantaneous reactive power is:

(8.b) $$w_B^n = \underline{\hat{u}}^p \circ \underline{i}_B^n = \\ = B_{23}\left(\hat{u}_1^{p\,2} + 2\,\hat{u}_2^p\,\hat{u}_3^p\right) + B_{12}\left(\hat{u}_3^{p\,2} + 2\,\hat{u}_1^p\,\hat{u}_2^p\right)$$

By equating term w^n in (4.b) and w_B^n in (8.b) we get:

(8.c) $$\begin{cases} N_B^n \cos\varphi^n = -3\sqrt{3}\,\dfrac{U^{p\,2}}{2\omega} B_{12} \\ N_B^n \sin\varphi^n = 3\,\dfrac{U^{p\,2}}{2\omega}\left(2B_{23} - B_{12}\right) \end{cases}$$

where $N_B^n = 3U^p I^p$ is total unbalanced power. Thus, given N_B^n, voltage phase α^p, and negative-sequence current phase β^n, the values of B_{12} and B_{23} are easily derived from (8.c). If they are both positive, the solution is acceptable. Otherwise, a common quantity is added to B_{12}, B_{23}, B_{31} to make two of them positive and the third zero. The corresponding equations can easily be derived from (8.b) and (8.c) by symmetry.

Let's assume, for simplicity, that the solution is acceptable. From (8.c) it's easy to show that:

$$\frac{B_{12}+B_{23}}{\omega} = \frac{2N_B^n}{3U^{p\,2}}\sin\left(\varphi^n - \pi/3\right)$$

The maximum value of total susceptance $B_{12}+B_{23}$ occurs if $\sin\left(\varphi^n - \pi/3\right) = 1$. In this case we have:

(9.a) $$B_{12} = B_{23} = B_B^n = \omega\frac{N_B^n}{3U^{p\,2}} \qquad B_{31} = 0$$

The reactive power absorbed by the *TCR* becomes:

(9.b) $$Q_{B\max}^n = 3U^{p\,2}\left(B_{12}+B_{23}\right) = 2\,N_B^n$$

Instead, the minimum total susceptance occurs when $\cos\varphi^n = 0$ in (8.c). Correspondingly we have:

(9.c) $$B_{23} = B_B^n = \omega\frac{N_B^n}{3U^{p\,2}}, \quad B_{12} = B_{31} = 0$$

and the reactive power absorbed by the *TCR* is:

(9.d) $$Q_{B\min}^n = N_B^n$$

The above relations have general validity, and do not depend on which susceptance is set to zero to make the computation. They show that compensation of unbalance power N_B^n requires a reactive power absorption by the *TCR* in the range $N_B^n \div 2\,N_B^n$. Moreover, the symmetrical susceptances which can be used for reactive power compensation are limited in the range:

(9.e) $$0 \le B_B^p \le B_{\max} - B_B^n$$

Correspondingly, the reactive power compensation capability of the *TCR* is reduced by $3\,N_B^n$.

Note finally that, since instantaneous power terms (4.b) are conservative, an unbalance power command can be sent remotely in the form:

(10) $$N_B = N_B\,e^{j\left(\alpha^p+\beta^n\right)}$$

This provides the information about N_B and $\alpha^p + \beta^n$, which are sufficient to drive the *TCR* provided that there is time synchronization between local and remote controllers. Given reactive power and unbalance power commands, *TCR* have the full information needed to perform reactive and unbalance compensation.

SPC operation and control

The switching units are capable of dynamic compensation, i.e., they can compensate for every power or current term (reactive, unbalance, void) also in presence of asymmetrical and distorted supply. For this purpose they

are driven by instantaneous power/energy vector references, in the form:

(10.a) $$[s] = [p \;\; w]$$

Power references [*s*] are then transformed into current references $\underline{i}^*$ by setting:

(10.b) $$\begin{cases} \underline{u} \circ \underline{i}^* = p^* \\ \underline{\hat{u}} \circ \underline{i}^* = w^* \\ \sum_{n=1}^{3} i_n^* = 0 \end{cases} \Rightarrow \underline{i}^* = \begin{vmatrix} u_1 & u_2 & u_3 \\ \hat{u}_1 & \hat{u}_2 & \hat{u}_3 \\ 1 & 1 & 1 \end{vmatrix}^{-1} \begin{vmatrix} p^* \\ w^* \\ 0 \end{vmatrix}$$

Current commands are then executed by *SPC* control according to usual current control techniques.

Fast Algorithm for Control Variables Estimation

The measurement of mean values of periodical signals at the line frequency (or twice the line frequency) is needed to compute unbiased integrals of voltages and currents, active power and reactive energy. With usual moving average filters the best achievable delay is *T/2*, where *T* is the line period. In the worst case, depending on the phase of input waveform, the delay can approach an entire period *T*. Hereafter, an recursive computation algorithm is proposed, which is faster than moving average and does not require extensive data storage and processing. Moreover, it is characterized by low computational complexity.

Let's consider a purely sinusoidal signal at the line frequency with non-zero average value, expressed by:

(11) $$x = X\cos(\omega t + \alpha) + c = \begin{vmatrix} \sin\omega t & \cos\omega t & 1 \end{vmatrix} \begin{vmatrix} a \\ b \\ c \end{vmatrix}$$

where ω is the angular frequency, c the average value of the signal, a and b the first coefficients of the Fourier series. In order to develop the estimation algorithm, note that coefficients *a, b, c* are easily obtained from (11). In fact, by multiplying both sides of (11) by the transpose of vector $\begin{vmatrix} \sin\omega t & \cos\omega t & 1 \end{vmatrix}$ and then integrating, we get:

(12.a) $$\int_0^t \begin{vmatrix} \sin\omega\tau \\ \cos\omega\tau \\ 1 \end{vmatrix} x(\tau)\,d\tau = \begin{vmatrix} a \\ b \\ c \end{vmatrix} \int_0^t D(\tau)\,d\tau = \begin{vmatrix} a \\ b \\ c \end{vmatrix} D_{\int}(t)$$

where:

(12.b) $$D(\tau) = \begin{vmatrix} \sin\omega\tau \\ \cos\omega\tau \\ 1 \end{vmatrix} \begin{vmatrix} \sin\omega t & \cos\omega t & \mathbf{1} \end{vmatrix}$$

It is easy to show that the 3x3 integral matrix $D_{\int}$ is singular only for $t=0$, and is invertible for each $t>0$. Expressing (12.a) in the discrete-time domain and then inverting we get a recursive estimation of coefficients a_k, b_k, c_k in the form:

(13) $$\begin{vmatrix} a_k \\ b_k \\ c_k \end{vmatrix} = D_{\int}^{-1}(kT_C) \sum_{n=0}^{k} \left(\begin{vmatrix} \sin\omega nT_C \\ \cos\omega nT_C \\ 1 \end{vmatrix} x(nT_C) \right), \quad \mathbf{k > 1}$$

where T_C is the sampling time. According to (13), the recursive estimation is updated at any sampling period. Note that the algorithm is independent on amplitude and initial phase of the signal, while it is dependent on line frequency ω. This limitation is overcome by synchronizing the algorithm with line frequency.

Inverse integral matrix anaysis

Integral matrix $D_{\int}$ is a function of references $\sin\omega t$ and $\cos\omega t$ sampled at every T_C. The inverse matrix can therefore be pre-calculated for each $k \neq 0$ and stored in a look-up table. From the analysis of the inverse integral matrix $D_{\int}^{-1}$ it follows that all matrix elements converge to constant values, giving a stable solution for coefficients *a, b, c*. The convergence time depends on the type of waveform and is discussed in the next paragraph.

Algorithm convergence time

As mentioned before, if the signal is purely sinusoidal the algorithm converges in a single computation step, independently of signal amplitude and phase. In practice, the algorithm performance is degraded in case of distorted signal or in presence of fundamental frequency variations.

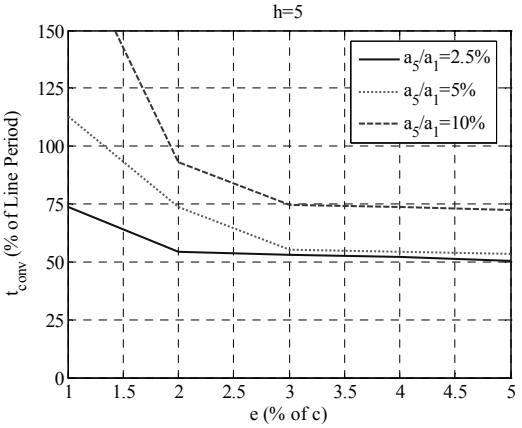

Fig. 2. Algorithm convergence time t_{conv} vs convergence error, e for different values of 5-th harmonic amplitude a_5

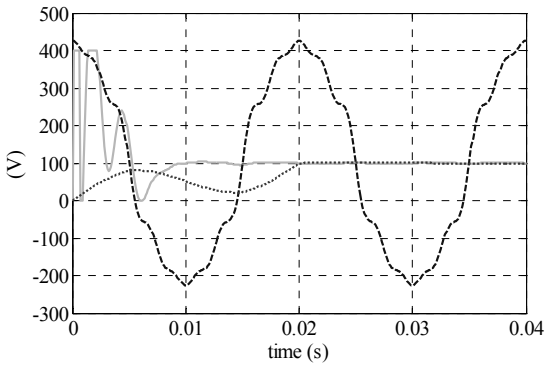

Fig. 3. Input voltage (dashed), Fast Algorithm output (continuos) and Moving Average Filter output (dotted) for initial phase $\varphi = \pi/2$.

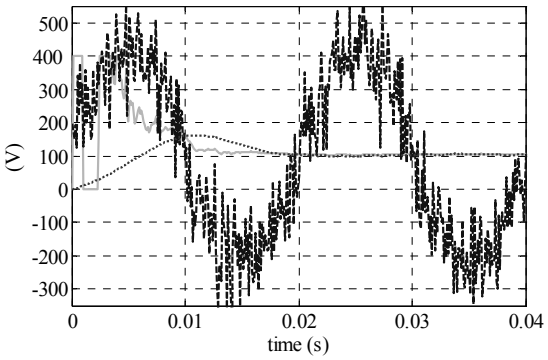

Fig. 4. Input voltage (dashed), Algorithm output (continuos) and Moving Average Filter output (dotted) for initial phase $\varphi=0$ and additive zero mean $\delta=20$ V Gaussian noise

The actual performance of the algorithm was tested by assuming that signal x in (13) includes a component x_f at the fundamental frequency f plus a single harmonic term x_h of amplitude a_h and frequency $f_h=h\ f$. The algorithm convergence time t_{conv} was analyzed as a function of a_h and f_h. As we are interested in determining the dc value c of signal x, the convergence time t_{conv} is defined as the instant at which the estimation of c enters in the allowed error band ($\pm e\%$). Since the algorithm is nonlinear, t_{conv} is a function of harmonic order h, amplitude a_h, mean value c, and error band $e\%$.

To illustrate the dependence of t_{conv} on the various parameters, Fig.2 shows the case of a 5-th harmonic superimposed to the fundamental component (amplitude a_1= 324V), assuming c = 100V. Note that the convergence time is approximately half a line period if an error between 3 and 5% is accepted and the harmonic amplitude is lower than 5% of the fundamental, while it tends to increase for higher accuracy or with higher harmonic content. For the other harmonics the behavior is similar, and it can be demonstrated that, given the harmonic amplitude a_h, t_{conv} decreases as the harmonic order increases.

In case of large line frequency variations t_{conv} may increase considerably if the algorithm is not synchronized. Instead, it performs efficiently if angular frequency ω in (12.b) is synchronized with actual line frequency.

Simulation results

The algorithm has been used to compute the average value of the unbiased integral of a voltage affected by a high distortion, as it can happen in smart micro-grids. The voltage integral includes a fundamental component (50 Hz, 230 Vrms), a set of odd harmonics (3-th to 9-th, each one set to 5% of the fundamental), and a dc term of 100V. The results of the estimation algorithm are shown in Figs.3 and 4, together with those achieved by a moving average filter, for different values of the initial phase and by adding also a Gaussian noise (Fig.4). The moving average filter has a convergence time which depends on dc value and initial phase, even in absence of harmonics, and is always between $T/2$ and T (line period). Instead, the proposed algorithm has a convergence time of few sampling periods in absence of harmonics and of approximately $T/2$ in presence of a considerable amount of harmonics.

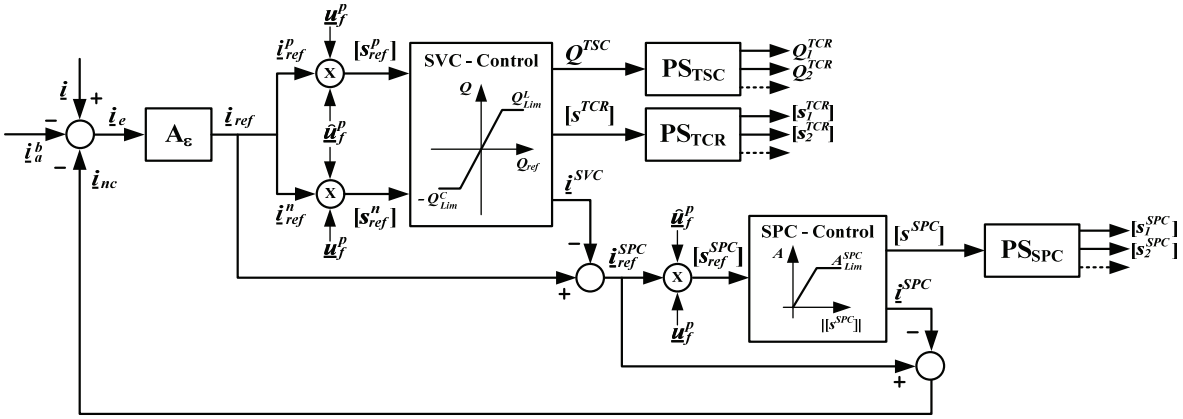

Fig. 5 - Concept scheme of distributed control

Cooperative Control of Distributed Electronic Power Processors

The general control structure of a system of distributed compensators is shown in Fig.5. The compensation aims at improving the power factor at the *PCC* by taking full advantage of the distributed compensation system. The controller performs as follows.

First of all, the current references at the *PCC* are determined. They coincide with the balanced active currents needed to meet the total power demand, i.e.:

$$\underline{i}_a^b = \frac{P}{U^2}\underline{u} \tag{14}$$

where P is the total power absorbed at the *PCC* and U is the collective rms value of *PCC* voltages $\underline{u}$. If the compensated network absorbs these currents the power factor becomes unity, as desired. The reference currents (detracted by *non-compensable current terms* $\underline{i}_{nc}$, which appear if the compensation capability of the system is saturated) are then compared with actual currents $\underline{i}$ absorbed at *PCC* to generate current errors $\underline{i}_e$. These latter are processed by the error amplifier, which produces internal current references $\underline{i}_{ref}$. These are then split into positive- and negative-sequence components and the corresponding fundamental components ($\underline{i}_{ref}^p, \underline{i}_{ref}^n$) are extracted. Let $\underline{u}^p$ be the positive-sequence voltage components at the fundamental frequency, the controller generates the power/energy vector command given by:

$$\begin{aligned}\left[s_{ref}^p\right] &= \left[p_{ref}^p \;\; w_{ref}^p\right] \\ \left[s_{ref}^n\right] &= \left[p_{ref}^n \;\; w_{ref}^n\right]\end{aligned} \tag{15}$$

These commands are then compared with actual reactive and unbalance compensation capability of *SVC* (which is updated dynamically by gathering information from distributed compensators) to generate the power/energy vector commands for the *TSC* (Q^{TSC}) and the *TCR* ($[s^{TCR}]$). The Power Sharing section of the controller (*PS*) distributes the power commands to the compensation units on the basis of their rated power, distance from the *PCC* and available compensation capability.

Based on the previous computations, the controller estimates the amount of compensated reactive and unbalance currents and, by difference, generates the current references $\underline{i}_{ref}^{SPC}$ for the *SPC*, which include also the void currents. References $\underline{i}_{ref}^{SPC}$ are then multiplied by $\underline{u}^p$ and $\widehat{\underline{u}}^p$ to generate power/energy vector command $\left[S_{ref}^{SPC}\right]$. Such power/energy command is then compared with the actual compensation capability of the *SPC* to generate the actual compensation command $\left[s^{SPC}\right]$, which

is then shared among the various compensation units. Finally, the non-compensable current terms, which exceed the total available compensation capability, are fed back to the current comparison node

Application Example

As an example of cooperative control the network of Fig. 6 was simulated. It includes unbalance and distorting loads, distribution lines, transformers, various compensation units (fixed capacitor bank, *TCR*, *APF*) and is fed by distorted and asymmetrical voltages. The central and local control units are implemented according to Fig. 5, with the goal to optimize the power factor at *PCC*.

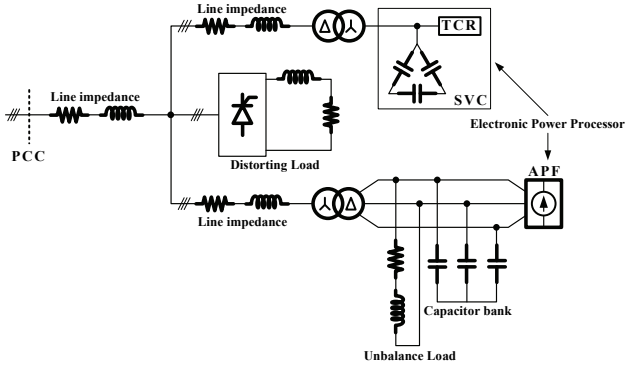

Fig. 6. Simulated Network

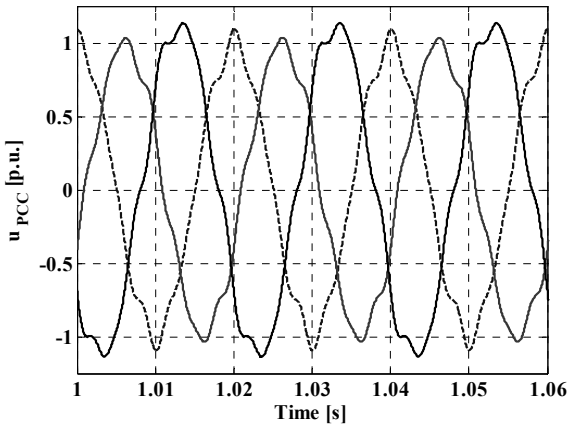

Fig. 7. Voltages at PCC

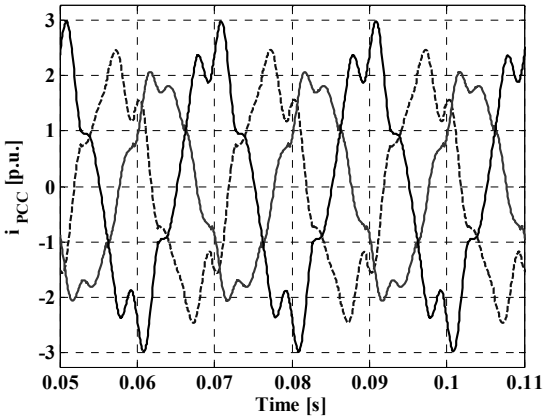

Fig. 8. Currents at PCC without compensation

The *TCR* is switched on at time t_1 (0.2 s) and the *APF* at time t_2 (0.6 s). Fig. 7 shows the voltages at *PCC*. They exhibit considerable asymmetry (unbalance factor: 10%) and distortion (5th harmonic: 5.0%; 7th harmonic: 5.0%). Fig. 8 shows the currents at PCC when the compensation units are off. The high distortion is due not only to the distorting load, but also to the capacitor bank located next to the *TCR*. The current asymmetry is due to load unbalance and voltage asymmetry. Fig. 9 shows the currents at *PCC* after time t_1 when the *SVC* is turned on. Although distorted, the fundamental components of the currents are now reasonably balanced and in phase with line voltages. Fig. 10 shows the currents at *PCC* after time t_2, when also the *APF* is turned on. Within the control bandwidth, the input currents now track active current references with good accuracy.

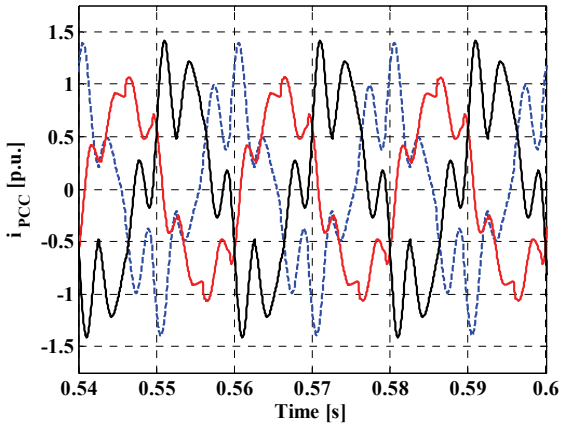

Fig. 9. Currents at PCC with SVC turned on

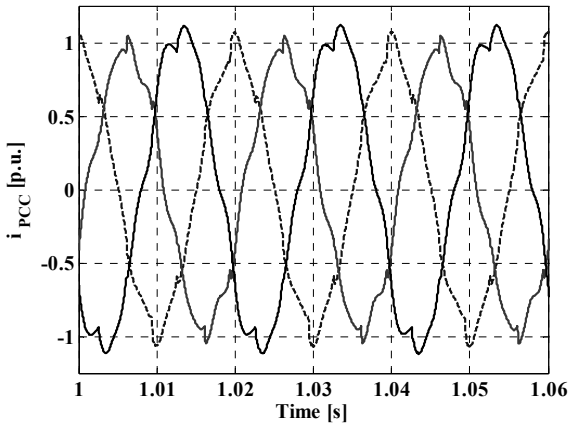

Fig. 10. Currents at PCC with SVC and APF turned on

Conclusions

A general approach to cooperative control of distributed electronic power processors acting in smart grids has been presented, which allows effective utilization of distributed compensation capability and energy resources. The approach makes use of the Conservative Power Theory both to define the compensation power under non-sinusoidal conditions and to control remote compensators by conservative power commands. Fast estimation algorithms have also been developed to speed up the dynamic response of the distributed compensation system. The proposed approach has been tested by simulation on a significant application example, showing excellent static and dynamic performance even in presence of severe distortion and unbalance in voltage supply and load currents.

REFERENCES

[1] Jintakosonwit P., Fujita H., Akagi H., Ogasawara S., "Implementation and Performance of Cooperative Control of Shunt Active Filters for Harmonic Damping Throughout a Power Distribution System" *IEEE Trans on Industry Applications*., 39(2003), No.2, pp. 556–563.

[2] Cheng P.T., Lee T. L., "Distributed active filter systems (DAFS): A new approach to power systems harmonics", *IEEE Trans. Ind. Applicat*, 42(2006), No. 5, pp. 1301-1309.

[3] Tedeschi E., Tenti P., Mattavelli P., Trombetti D., "Cooperative control of electronic power processors in micro-grid", *Brasilian Transactions on Power Electronics*, 14(2008), No. 4., pp. 241-249.

[4] Czarnecki L.S., "Reactive and unbalanced currents compensation in three-phase asymmetrical circuits under non-sinusoidal conditions" *IEEE Trans. on Instrumentation and Measurements*, 38(1989), pp. No3., 754-759.

[5] Czarnecki L.S., "Power factor improvement of three-phase unbalanced loads with nonsinusoidal supply voltages", *European Trans. on Electrical Power Engineering (ETEP)*, 3(1993), No. 1, pp. 67-72.

[6] Tenti P., Trombetti D., Tedeschi E., Mattavelli P., "Compensation of load unbalance, reactive power and harmonic distortion by cooperative operation of distributed compensators", *European Conference on Power Electronics and Drives*, Barcelona, 2009.

[7] Akagi H., "Control strategy and site selection of a shunt active filter for damping of harmonic propagation in power distribution systems," *IEEE Trans. Power Delivery*, 12(1997), pp. 354–363.

[8] Tenti P., Mattavelli P., Morales P H. K, "Conservative Power Theory, Sequence Components and Accountability in Smart Grids" *Przeglad Elektrotechniczny*, 6(2010), pp. 30-37.

[9] Gyugyi L., Otto R.A., Putman T.H., "Principles and applications of static, thyristor-controlled, shunt compensators", *IEEE Transactions on Power Apparatus and Systems*, 97(1978), No. 5 pp. 1935-1945.

[10] Tenti P., Willems J.L., Mattavelli P., Tedeschi, E., "Generalized Symmetrical Components for Periodic Non-Sinusoidal Three-Phase Signals", *Seventh International Workshop on Power Definition and Measurements under Nonsinusoidal Conditions*, Cagliari (Italy), July 2006.

[11] Mattavelli P., "A closed-loop selective harmonic compensation for active filters", *IEEE Trans. Industry Applications*, 37(2001), No. 1, pp. 81-89.

[12] Page C.H., "Reactive Power in Non-Sinusoidal Situations", *IEEE Trans. of Instrumentation and Measurement*, 29(1990), No.4, pp. 420-423.

[13] Czarnecki, L.S., "Scattered and reactive current, voltage, and Power in Circuits with nonsinusoidal waveforms and their compensation". *IEEE Trans. on Instrumentation and Measurements*, 40(1991), No.3, pp. 563-567.

[14] Czarnecki, L.S., "Minimization of Reactive Power under Nonsinusoidal Conditions", *IEEE Trans. on Instrumentation and Measurements*, 36(1987), No.1, pp. 18-22.

[15] Merhej S.J., Nichols W.H., "Harmonic Filtering for the Offshore Industry", *IEEE Trans. on Industry Applications*, 30(1994), No. 3, pp. 533-542.

[16] Akagi H., Kanazawa Y., Nabae A., "Instantaneous reactive power compensators comprising switching devices without energy storage components", *IEEE Trans. Ind. Appl*., 20(1984), No. 3, pp. 625-630.

[17] Akagi H., Nabae A., "Control Strategy of Active Power Filters Using Multiple Voltage Source PWM Converters", *IEEE Trans. on Ind. App*., 22(1986), No. 3, pp.460-465.

[18] Depenbrock M., Marshall D.A., Van J.D. Wyk: "Formulating Requirements for a Universally Applicable Power Theory as Control Algorithm in Power Compensators", *European Trans. on Electrical Power Engineering (ETEP)*, 4(1994), No. 6, pp. 445-455.

[19] Willems J.L., "Mathematical foundations of the instantaneous power concept: a geometrical approach", *European Trans. on Electrical Power, ETEP*, 6(1996), No. 5, pp. 299-304.

***Authors**: Dr. Helmo K. Morales Paredes, School of Electrical and Computer Engineering, Department of Electrical Energy Systems, University of Campinas, Unicamp/FEEC/DSEE, Av. Albert Einstein, 400, 13083-852 Campinas, SP – Brazil, hmorales@dsee.fee.unicamp.br. Dr. Alessandro Costabeber, Department of Information Engineering University of Padova, Via Gradenigo 6/B, 35131 Padova Italy, E-mail costabeber@dei.unipd.it, Prof. Paolo Tenti, Department of Information Engineering University of Padova, Via Gradenigo 6/B, 35131 Padova Italy, E-mail paolo.tenti.@unipd.it;*